

Rotation Periods of Young Brown Dwarfs: K2 Survey in Upper Scorpius

Alexander Scholz¹, Veselin Kostov², Ray Jayawardhana³, Koraljka Mužić^{4,5}
as110@st-andrews.ac.uk

ABSTRACT

We report rotational periods for 16 young brown dwarfs in the nearby Upper Scorpius association, based on 72 days of high-cadence, high-precision photometry from the *Kepler* space telescope's K2 mission. The periods range from a few hours to two days (plus one outlier at 5 days), with a median just above one day, confirming that brown dwarfs, except at the very youngest ages, are fast rotators. Interestingly, four of the slowest rotators in our sample exhibit mid-infrared excess emission from disks; at least two also show signs of disk eclipses and accretion in the lightcurves. Comparing these new periods with those for two other young clusters and simple angular momentum evolution tracks, we find little or no rotational braking in brown dwarfs between 1-10 Myr, in contrast to low-mass stars. Our findings show that disk braking, while still at work, is inefficient in the substellar regime, thus provide an important constraint on the mass dependence of the braking mechanism.

Subject headings:

1. Introduction

Rotation is a key parameter in stellar evolution, and is directly linked to many fundamental astrophysical processes, including magnetic field generation, stellar winds, star-disk interaction, and binary formation (Herbst et al. 2007; Bouvier et al. 2014). Because rotation drives magnetic activity, it is also relevant for 'space weather' in the stellar surroundings and thus for planetary habitability (Güdel 2007; Vidotto et al. 2014). The rotation period, derived from the periodic photometric

modulation induced by surface spots, is one of the rare stellar parameters that can be measured with high precision ($\sim 1\%$) for large samples.

Large numbers of periods have been measured for low-mass stars with spectral types F to M of all ages from ~ 1 Myr to several Gyrs (e.g. Herbst et al. 2002; Lamm et al. 2005; Irwin et al. 2008; McQuillan et al. 2014), and they provide very useful constraints for angular momentum evolution models (e.g. Gallet & Bouvier 2015). Other portions of the mass-age parameter space are still poorly explored. One example is the regime of BDs, substellar objects with masses less than $\sim 0.08 M_{\odot}$. The only regions with significant samples of measured BD periods are clusters in Orion, the ONC (Rodríguez-Ledesma et al. 2009) σ Ori (Scholz & Eislöffel 2004; Cody & Hillenbrand 2010), and ϵ Ori (Scholz & Eislöffel 2005), at ages of 1-5 Myr. Like stars, BDs start with a range of periods from hours up to 5-10 days, and spin up due to pre-main sequence contraction, but in contrast to stars they maintain fast rotation with negligible spindown for several Gyrs.

Due to their intrinsic faintness, the small pho-

¹School of Physics and Astronomy, University of St Andrews, North Haugh, St Andrews, Fife KY16 9SS, United Kingdom

²Department of Astronomy & Astrophysics, University of Toronto, 50 St. George Street, Toronto, ON M5S 3H4, Canada

³Faculty of Science, York University, 355 Lumbers Building, 4700 Keele Street, Toronto, ON M3J 1P2, Canada

⁴Nucleo de Astronomía, Facultad de Ingeniería, Universidad Diego Portales, Av. Ejercito 441, Santiago, Chile

⁵European Southern Observatory, Alonso de Córdova 3107, Casilla 19, Santiago 19001, Chile

tometric amplitudes, and the wide range of periods at young ages, it is challenging to obtain a reliable picture of the rotational evolution of BDs with ground-based observations alone, which feature typical daytime gaps and are therefore biased in the period sensitivity. There are good indications that disk braking is less efficient in the very low mass regime (e.g. Lamm et al. 2005). But the lack of substantial and unbiased period samples for a range of ages prohibits us from putting firm constraints on models.

Here we present first period measurements for BDs obtained with Kepler’s K2 mission (Howell et al. 2014). In campaign 2, the K2 field included large parts of the Upper Scorpius (UpSco) star forming region (age 5-10 Myr), which harbours a huge population of BDs (e.g. Lodieu et al. 2008; Slesnick et al. 2008; Lodieu et al. 2011; Dawson et al. 2014). With a cadence of 30 min and a time baseline of 72 d, the K2 lightcurves cover the entire period range for young BDs. During the course of its mission, K2 is expected to fill the period-age diagram for BDs with dozens of new datapoints; this study is the first step towards a new census of BD rotation.

2. Data processing

We observed brown dwarfs¹ in UpSco as part of campaign 2 of the K2 mission. The targets were selected from the census by Dawson et al. (2013) based on the UKIDSS survey. Analysis of mid-infrared data shows that $\sim 20\%$ still harbour circum-sub-stellar disks. 51 of the full sample of 116 have been covered by K2.

We downloaded the data, in the form of long-cadence target pixel files, from the Mikulsi Archive for Space Telescopes (MAST). To extract aperture photometry, detrend and correct for systematic effects we used the latest version of PyKE (Still & Barclay 2012). This is an open-source PyRAF package originally designed for custom manipulation of the *Kepler* data and now also including the self-flat-fielding procedure of Vanderburg & Johnson (2014) optimized for processing data from the K2 mission. The procedure utilizes the relation between the position of the target on the detec-

tor and the measured flux to correct for artifacts induced by the pointing drift of the spacecraft.

Our data reduction proceeds as follows. First we used PyKE’s *kepmask* to define sub-image apertures ($\sim 2 - 3 \times 2 - 3$ pixels) from the respective target’s postage stamp image (typically $10 - 12 \times 10 - 12$ pixels), then extract simple aperture photometry (SAP) with *kepxtract*. Next, we detrend and normalize the raw lightcurves with *kepflatten* using a low-order polynomial ($n \sim 3 - 5$) and, finally, to correct for the motion-induced systematic effects we use *kepsff*. As an illustrative example, on Fig. 1 we show a section of the SAP lightcurve (background-corrected) of EPIC204614722 (top panel), the two moment centroids (middle panels) and the corresponding *kepsff*-corrected lightcurve (lower panel). Throughout the data-reduction process we appropriately adjust the relevant input parameters on a target-by-target basis. We note that we used the entire campaign 2 dataset, including the majority of cadences from the second half of the campaign where most of the data flags are non-zero due to the photometer’s local detector electronics parity errors, as these do not affect the quality of the data for the purposes of detecting rotational variability.

3. Lightcurve analysis

All 51 lightcurves were visually inspected. 16 of them show clear signs of periodic variability. In most cases the periodicity is obvious and periods ranging from a few hours up to 5 d are estimated by eye. To measure the periods, we used the autocorrelation function, which has been established as a useful tool for period analysis in Kepler lightcurves by McQuillan et al. (2014). Compared to Fourier (Lomb-Scargle) or phase-based techniques (e.g., phase dispersion minimisation), it has the advantage that it is robust against phase/amplitude changes as well as systematics.

After dividing the lightcurves in seven segments of 500 datapoints each, each covering about 10 d with a uniform cadence of 30 min, we calculate the autocorrelation function and determine the position of the first non-zero peak, which is a measurement of the fundamental period in the dataset. For 10 objects, we find a consistent period in all 7 segments, for 5 more the same period is found

¹Some of our objects may be very low mass stars with masses slightly above the substellar limit; for convenience we will call all targets brown dwarfs.

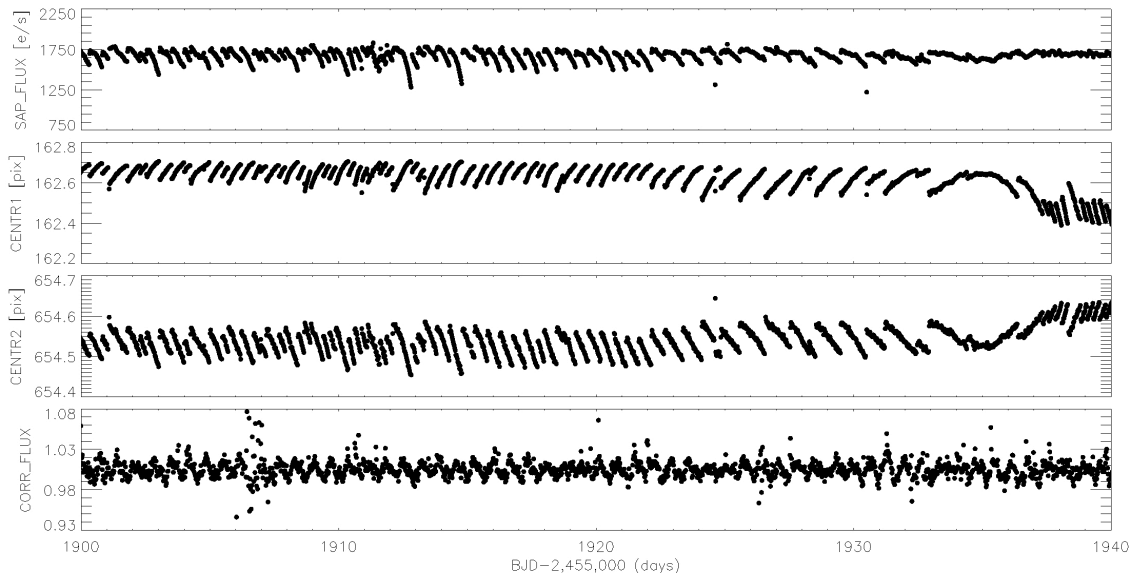


Fig. 1.— Processing of the SAP lightcurve for EPIC204614722, see text for details.

for 5 or 6 segments. The scatter in the individual period measurements is 1-8%, which we adopt as the uncertainty. One additional object shows an obvious ~ 5 d period, but also strong additional variations, which could be intrinsic to the object, but might also be partly instrumental. The best periods and the uncertainties are listed in Table 1. The lightcurves are plotted in phase to the best period (for the first 10 days of the campaign) in Fig. 2.²

To check for false positive signals due to contamination from other sources, we extracted the light curves of K2 stars near our targets as listed in MAST (typically much brighter, and within $\sim 2 - 3''$). We also tested various apertures on a target-by-target basis – from the central pixels, from the pixels surrounding them, and from any other conspicuously bright pixel in their respective postage stamp images – and visually examined the extracted light curves. Our analysis indicates that the flux modulations in our targets’ light curves originate in their respective central pixels only.

²We note that we find a period of $0.48 d$ for three targets not in Table 1, EPIC204367193, EPIC204418005, and EPIC204086791. We discard these because the lightcurves, phase plots and autocorrelation functions do not look convincing. These could be residuals of the systematics and have to be re-examined when new software is available.

In addition, with the exception of Mars moving across the detector containing our targets for a few days in October of 2014, there are no obvious false positive sources. We also confirmed that the periods estimated here are also visible in the lightcurves made publicly available by Vanderburg & Johnson (2014)³. Therefore we are convinced that the periods in Table 1 are of astrophysical origin.

The measured periods range from 0.2 to 5 d, with a median of 1.1 d. The amplitudes of the lightcurves are typically a few percent, with the shape usually well approximated by a sinus curve. According to spectroscopy analysed in the literature, the objects with measured periods have spectral types of M5 to M7.5 and effective temperatures from 2500 to 3000 K (Slesnick et al. 2008; Lodieu et al. 2011), corresponding to masses of 0.02 to $0.09 M_{\odot}$ (Baraffe et al. 2015). The majority of these objects are likely at the high end of this mass range. Given that our targets are all mid to late M dwarfs and thus magnetically active objects, the most straightforward explanation for the periodicities are magnetically induced cool spots on the surface, which modulate the flux over a rotational cycle. Therefore, we interpret the

³<https://www.cfa.harvard.edu/~avanderb/k2.html>

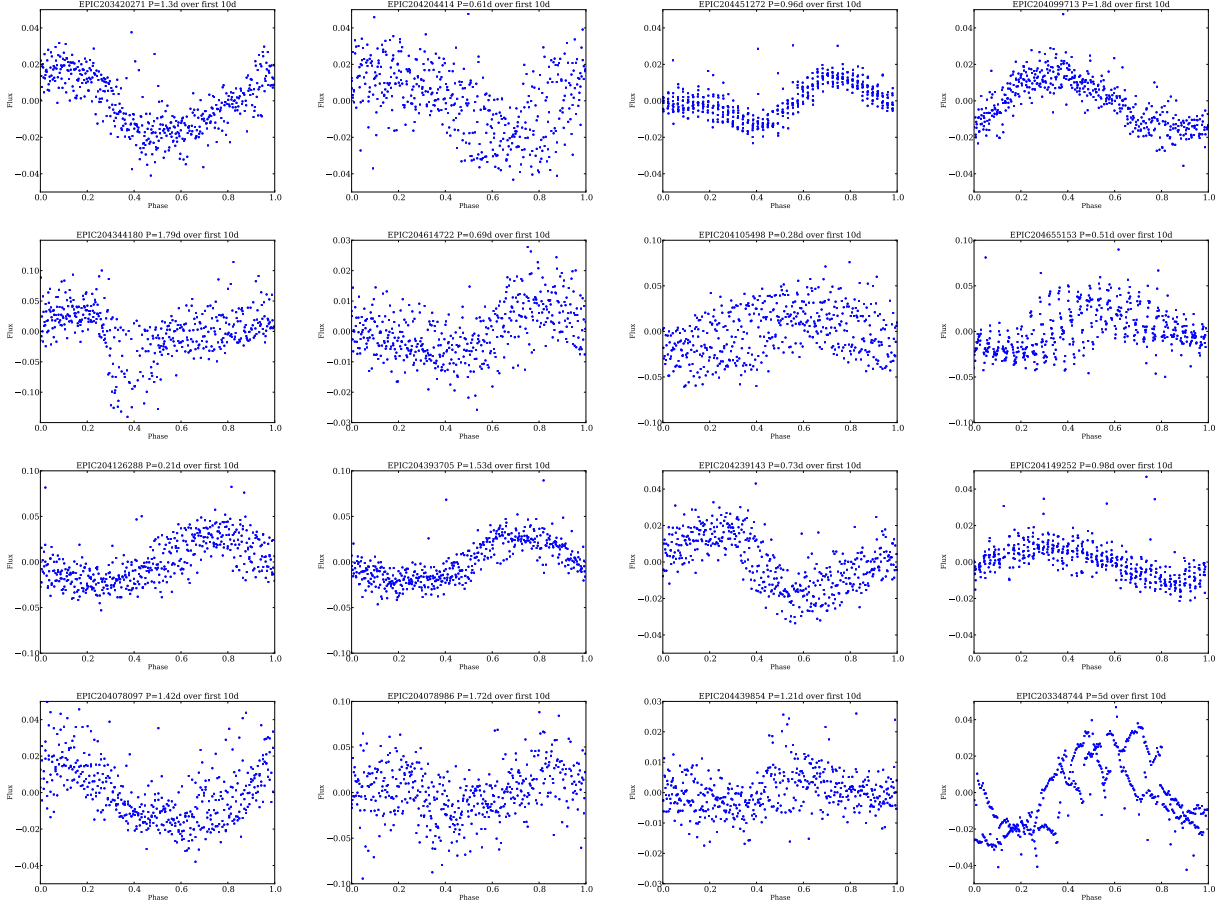


Fig. 2.— Phased lightcurves for the first ten days of the K2 campaign 2 for the 16 objects with detected periods, in the same order as in Table 1.

Table 1: UpSco rotation periods.

EPIC	2MASS	Kmag	T_{eff} (K) ^d	P (d)	Perr (d)
203420271	16033799-2611544	15.167		1.30	0.01
204204414	16153648-2315175	16.417	3025	0.61	0.02
204451272	16082229-2217029	15.556	3025	0.96	0.02
204099713	16112630-2340059	15.971	2818, 3025	1.80	0.03
204344180	16143287-2242133	16.775	2630, 2935	1.79	0.06 ^{a,b}
204614722	16095217-2136277	13.933	2570	0.66	0.03
204105498	16124692-2338408	14.964	2754, 2910	0.28	0.02
204655153	16105499-2126139	15.316	2754	0.51	0.01
204126288	16164539-2333413	16.293	2884, 3025	0.21	0.01
204393705	16132665-2230348	16.123	2910	1.53	0.03
204239143	16113837-2307072	15.143	2910	0.73	0.02
204149252	16133476-2328156	14.843	3025	0.98	0.02
204078097	16095852-2345186	13.992	2935	1.42	0.04 ^{a,c}
204078986	16080745-2345055	15.786	2935	1.72	0.08 ^a
204439854	16113470-2219442	14.662	2035	1.21	0.05
203348744	16030235-2626163	14.614		~ 5	0.5 ^a

^amid-infrared excess emission^birregular eclipses in the first part of the lightcurve^crapid amplitude changes^dreferences for T_{eff} : Slesnick et al. (2008), Lodieu et al. (2011)

periods as rotation periods. For a more detailed discussion on the causes of periodic variability in very low mass objects, see Scholz & Eislöffel (2004, 2005).

For the other 35 objects in the sample we cannot determine rotation rates. It is conceivable that the periods measured here are biased, particularly since we are using an activity phenomenon (spots) to derive periods, and activity may depend on rotation. Ultimately this can only be tested by complementary, activity-independent measurements of rotation, such as spectroscopic $v \sin i$. At this point there is no evidence for a bias in the photometric period samples; the rotation-activity relation is flat in mid M dwarfs and so far $v \sin i$ have confirmed the fast rotation of very low mass objects (e.g. Jackson & Jeffries 2012). Therefore, for the remainder of the paper we will assume that these periods are representative of young BDs in UpSco.

The periods are persistent throughout the campaign, i.e. over at least 72 d, with stable amplitudes. Most objects show clear signs of phaseshift: If we plot the datapoints as function of phase for each of the segments, the maximum shifts through

the observing campaign by 0.1-0.5 cycles over the course of 72 d. Comparing the phased lightcurve for various segments also shows in some cases indications for changes in the shape. Thus, while the surfaces of our targets are continuously covered by spots, the parts of the surfaces that induce the variability change over time. This is evidence for evolving spot pattern on young BDs. In one case (EPIC204614722) the period significantly decreases over the observing campaign, from 0.69 d to 0.61 d, most likely because the variability is induced by spots located at varying and differentially rotating latitudes.

Out of the 16 objects, 4 have mid-infrared colour excess indicating the presence of a disk (Class II, Dawson et al. 2013); the remainder are disk-less based on their broadband colours (Class III). One of the Class II sources, EPIC204344180, shows a series of eclipses in the first part of its lightcurve (Fig. 3, left panel). The width and depth of the features vary slightly, and the eclipses disappear after about 20 d. The dominant periodicity, however, persists over the entire lightcurve. This object might belong to the object class of AA-Tau analogs, recently termed 'dippers', which

show either regular or irregular eclipses, presumably caused by a wall at the inner edge of the disk (Morales-Calderón et al. 2011; Stauffer et al. 2015). To our knowledge, this is the first example of a BD ‘dipper’. The fact that the rotation period of this object is consistent with the period of the eclipses indicates that the disk feature has to be near co-rotation radius. Another one of the sources with disk, EPIC204078097, has only insignificant colour excess at $3\text{--}5\ \mu\text{m}$, but clearly exceeds the photospheric emission at $12\ \mu\text{m}$, which makes this a BD transition disk. This object shows irregular amplitude changes throughout the observing campaign (Fig. 3, right panel), possibly due to short accretion bursts, maybe analogous to the ones reported for stars by Stauffer et al. (2014) and Findeisen et al. (2013). As pointed out above, EPIC203348744, another Class II object, features irregular variability which could at least partially be caused by accretion or the presence of a disk.

4. Discussion

The new periods for UpSco BDs give us an opportunity to probe the rotational evolution in the substellar regime. At ages of 1–20 Myr, stars spin up when angular momentum is conserved, because they contract towards their final main-sequence radii. Angular momentum losses occur either due to magnetic star-disk coupling or accretion powered stellar winds (Matt et al. 2010, 2012). For a review of these processes and the observational evidence for disk braking, see Bouvier et al. (2014).

In Fig. 4 we compare the rotation periods in UpSco presented in this paper (Table 1) with the two other sizable samples of BD periods, in the ONC (Rodríguez-Ledesma et al. 2009) and σ Ori⁴ and with simple rotational evolution tracks. The models are calculated based on the evolutionary models by Baraffe et al. (2015), for a fiducial BD mass of $0.07\ M_{\odot}$. Adopting a different mass ($0.04\text{--}0.07\ M_{\odot}$) shifts the tracks slightly. All tracks assume angular momentum conservation. We also overplot the physical barrier for the rotation period (‘breakup period’).

For σ Ori, we combine the samples by Scholz & Eislöffel (2004) and Cody & Hillenbrand (2010). We also include in the σ Ori sample the BD peri-

ods for the cluster around ϵ Ori (Scholz & Eislöffel 2005), a poorly characterised region, but note that their inclusion does not change any of the following results. For the samples by Rodríguez-Ledesma et al. (2009) and Cody & Hillenbrand (2010) we adopt a magnitude cutoff of $I = 16.5$ to separate BDs from stars; this is subject to uncertainties in evolutionary tracks and cluster distances. For the other two samples, masses have been determined by comparing the IJHK photometry with evolutionary tracks in the original papers. In total we use 179 periods in the ONC and 29 periods in σ Ori. We overplot the median and the 10% and 90% percentile. All samples should be sensitive to periods ranging from ~ 0.2 to several days, in the case of the K2 sample up to several weeks.

The choice for the ages of σ Ori and UpSco is relevant for the discussion. For σ Ori members the plausible age range is 3–6 Myr (Sherry et al. 2008; Bell et al. 2013), for UpSco 5–12 Myr (Preibisch et al. 2002; Pecaute et al. 2012). Both regions are significantly older than the ONC, and UpSco is probably again significantly older than σ Ori. In Fig. 4 we choose ages of 4 and 8 Myr for σ Ori and UpSco, respectively. Age spread is probably present in both regions, but since ages for individual BDs are not easily determined, this is neglected here.

The median and percentiles for the UpSco periods are slightly lower than in the ONC, consistent with spinup due to contraction. Compared with σ Ori, the median and lower limit are actually slightly higher in UpSco. We do not put too much emphasis on this finding at this point, since we cannot be sure that we are not missing some of the ultrashort periods in the K2 lightcurves, which may have been removed together with systematics. The upper limit in UpSco is lower than in σ Ori, mostly because σ Ori has a larger fraction of slow rotators with $P > 2\ d$ (8/29 vs. 1/16). Some of the periods in σ Ori and ϵ Ori are below or very close to the breakup period, this may have consequences on the rotational evolution, see discussion in Scholz & Eislöffel (2005).

From Fig. 4 it is evident that the current period census does not require any disk braking to explain the evolution of the period median and upper/lower limits. Only ages at the upper end of the plausible range (6 Myr for σ Ori, 11 Myr for UpSco) may require to include some disk locking in the evolutionary tracks, but only for the

⁴Joergens et al. (2003) published 3 more periods for young BDs in Chamaeleon-I (age 1–2 Myr), with $P = 2.2 \dots 3.4\ \text{d}$.

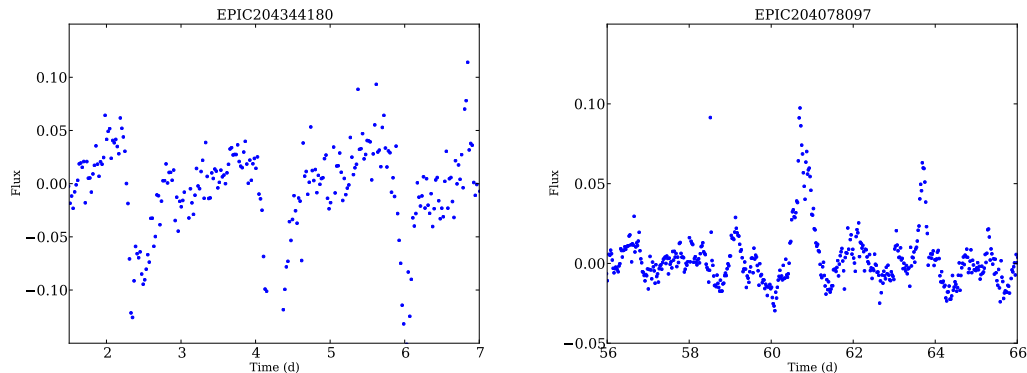


Fig. 3.— Partial lightcurves for two objects with periodic variability to highlight the irregular eclipses (EPIC204344180, left panel) and bursts (EPIC204078097, right panel).

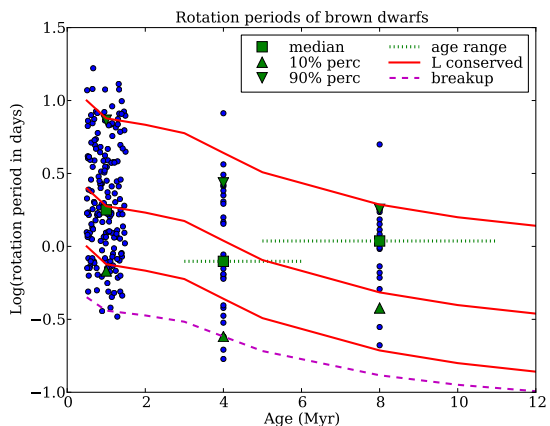


Fig. 4.— Rotation periods for brown dwarfs as a function of age, compared with evolutionary tracks assuming angular momentum conservation. The breakup period is plotted as well. The periods at 1 Myr (ONC) are randomly spread out in age for clarity.

slow rotators and only over a locking timescale of $< 2 - 3$ Myr. This is about half as long as the locking timescale for slowly rotating low-mass stars (Herbst & Mundt 2005; Gallet & Bouvier 2013). Thus, independent of the choice of the ages, this analysis robustly demonstrates that disk braking is inefficient in the BD regime. This is consistent with earlier findings of ‘moderate angular momentum loss’ in very low mass stars, by Lamm et al. (2005). It is notable that the four objects with disk in the UpSco sample are among the six slowest rotators, with periods of 1.4, 1.7, 1.8 d, and 5 d well above the median. This indicates that disk braking does have some effect, but only for very few objects and/or on short timescales.

5. Summary

We have measured a sample of rotation periods for young brown dwarfs in the UpSco region, using lightcurves from campaign 2 of the K2 mission. Our periods range from a few hours up to 5 d, with a median just above one day, confirming that BDs, except at the youngest ages, are fast rotators. Four of the slowest rotators have mid-infrared excess emission due to the presence of a disk; at least two of them show signs of disk eclipses and accretion in the lightcurves. We compare the new periods with previously published samples in the ONC and σ Ori and show that the period evolution from 1 to 10 Myr is consistent with no or little rotational braking, in contrast to low-mass stars. This confirms that disk braking, while still at work, is inefficient in the BD regime. This main

finding is potentially an important constraint on the mass dependence of the braking mechanism. Compared with low-mass stars, young BDs have much lower accretion rates (e.g. Natta et al. 2004), weak magnetic fields (Reiners et al. 2009), and possibly lower ionisation rates at the inner edge of the gas disk. These characteristics may influence the efficiency of rotational braking.

We thank Thomas Barclay for his assistance with PyKE and Andrew Vanderburg for a fruitful discussion on the details of his data reduction technique. This work was supported in part by NSERC grants to R. Jayawardhana. This work made use of PyKE (Still & Barclay 2012), a software package for the reduction and analysis of Kepler data. This open source software project is developed and distributed by the NASA Kepler Guest Observer Office.

REFERENCES

- Baraffe, I., Homeier, D., Allard, F., & Chabrier, G. 2015, *A&A*, 577, A42
- Bell, C. P. M., Naylor, T., Mayne, N. J., Jeffries, R. D., & Littlefair, S. P. 2013, *MNRAS*, 434, 806
- Bouvier, J., Matt, S. P., Mohanty, S., et al. 2014, *Protostars and Planets VI*, 433
- Cody, A. M., & Hillenbrand, L. A. 2010, *ApJS*, 191, 389
- Dawson, P., Scholz, A., Ray, T. P., et al. 2013, *MNRAS*, 429, 903
- Dawson, P., Scholz, A., Ray, T. P., et al. 2014, *MNRAS*, 442, 1586
- Findeisen, K., Hillenbrand, L., Ofek, E., et al. 2013, *ApJ*, 768, 93
- Gallet, F., & Bouvier, J. 2013, *A&A*, 556, A36
- Gallet, F., & Bouvier, J. 2015, *A&A*, 577, A98
- Güdel, M. 2007, *Living Reviews in Solar Physics*, 4, 3
- Herbst, W., Bailer-Jones, C. A. L., Mundt, R., Meisenheimer, K., & Wackermann, R. 2002, *A&A*, 396, 513
- Herbst, W., & Mundt, R. 2005, *ApJ*, 633, 967
- Herbst, W., Eisloffel, J., Mundt, R., & Scholz, A. 2007, *Protostars and Planets V*, 297
- Howell, S. B., Sobek, C., Haas, M., et al. 2014, *PASP*, 126, 398
- Irwin, J., Hodgkin, S., Aigrain, S., et al. 2008, *MNRAS*, 383, 1588
- Jackson, R. J., & Jeffries, R. D. 2012, *MNRAS*, 423, 2966
- Joergens, V., Fernández, M., Carpenter, J. M., & Neuhäuser, R. 2003, *ApJ*, 594, 971
- Lamm, M. H., Mundt, R., Bailer-Jones, C. A. L., & Herbst, W. 2005, *A&A*, 430, 1005
- Lodieu, N., Hambly, N. C., Jameson, R. F., & Hodgkin, S. T. 2008, *MNRAS*, 383, 1385
- Lodieu, N., Dobbie, P. D., & Hambly, N. C. 2011, *A&A*, 527, A24
- Matt, S. P., Pinzón, G., de la Reza, R., & Greene, T. P. 2010, *ApJ*, 714, 989
- Matt, S. P., Pinzón, G., Greene, T. P., & Pudritz, R. E. 2012, *ApJ*, 745, 101
- McQuillan, A., Mazeh, T., & Aigrain, S. 2014, *ApJS*, 211, 24
- Morales-Calderón, M., Stauffer, J. R., Hillenbrand, L. A., et al. 2011, *ApJ*, 733, 50
- Natta, A., Testi, L., Muzerolle, J., et al. 2004, *A&A*, 424, 603
- Pecaut, M. J., Mamajek, E. E., & Bubar, E. J. 2012, *ApJ*, 746, 154
- Preibisch, T., Brown, A. G. A., Bridges, T., Guenther, E., & Zinnecker, H. 2002, *AJ*, 124, 404
- Reiners, A., Basri, G., & Christensen, U. R. 2009, *ApJ*, 697, 373
- Rodríguez-Ledesma, M. V., Mundt, R., & Eisloffel, J. 2009, *A&A*, 502, 883
- Scholz, A., & Eisloffel, J. 2004, *A&A*, 419, 249
- Scholz, A., & Eisloffel, J. 2005, *A&A*, 429, 1007

- Scholz, A., Eislöffel, J., & Mundt, R. 2009, MNRAS, 400, 1548
- Sherry, W. H., Walter, F. M., Wolk, S. J., & Adams, N. R. 2008, AJ, 135, 1616
- Slesnick, C. L., Hillenbrand, L. A., & Carpenter, J. M. 2008, ApJ, 688, 377
- Stauffer, J., Cody, A. M., Baglin, A., et al. 2014, AJ, 147, 83
- Stauffer, J., Cody, A. M., McGinnis, P., et al. 2015, AJ, 149, 130
- Still, M., & Barclay, T. 2012, Astrophysics Source Code Library, 1208.004
- Vanderburg, A., & Johnson, J. A. 2014, PASP, 126, 948
- Vidotto, A. A., Jardine, M., Morin, J., et al. 2014, MNRAS, 438, 1162